Eur. Phys. J. D **38**, 515–522 (2006)
DOI: 10.1140/epjd/e2006-00059-5

THE EUROPEAN PHYSICAL JOURNAL D

Optical study of radicals (OH, O, H, N) in a needle-plate bi-directional pulsed corona discharge

F. Liu, W. Wang[a], W. Zheng, and Y. Wang

State Key Laboratory of Materials Modification by Laser, Ion and Electron Beams, Dalian University of Technology, Dalian 116024, P.R. China

Received 17 November 2005 / Received in final form 16 January 2006
Published online 21 March 2006 –

Abstract. In this study, analysis of optical emission spectra are used for the detection of OH ($A^2\Sigma$) radicals and O ($3p^5P$), H_α (3P) and N ($3p^4P$) active atoms produced by the high-voltage bi-directional pulsed corona discharge of N_2 and H_2O mixture gas in a needle-plate reactor at one atmosphere. The relative vibrational populations and the vibrational temperature of N_2 (C, v') are determined. The effects of pulse peak voltage, pulse repetition rate and the added O_2 flow rate on the relative populations of OH ($A^2\Sigma$) radicals and O ($3p^5P$), H_α (3P) and N ($3p^4P$) active atoms are investigated. It is found that when pulse peak voltage and pulse repetition rate are increased, the relative populations of those excited states radicals rise correspondingly. The relative population of OH ($A^2\Sigma$) radicals decreases with increasing the flow rate of oxygen. The relative populations of O ($3p^5P$), H_α (3P) and N ($3p^4P$) active atoms increase with the flow rate of oxygen at first and exhibit a maximum value at about 30 ml/min. When the flow rate of oxygen is increased further, the relative populations of those excited states active atoms decrease correspondingly. The main involved physicochemical processes also have been discussed.

PACS. 52.70.Kz Optical (ultraviolet, visible, infrared) measurements – 52.80.Hc Glow; corona – 82.33.Xj Plasma reactions (including flowing afterglow and electric discharges) – 52.20.Hv Atomic, molecular, ion, and heavy-particle collisions

1 Introduction

Pulsed corona discharge is one of non-thermal plasma characterized by low gas temperature and high-electron temperature. Short-duration pulsed corona discharge has some advantages over other method, which is more efficient in energy conversion than other non-thermal plasma techniques. By pulsed corona discharge, more electrical energy input goes into the production of energetic electrons than gas heating [1]. High-energy electrons generated by short-duration pulsed corona discharge can efficiently dissociate, excite and ionize N_2, O_2 and H_2O into oxygenated radicals (OH, O, H, N, HO_2, etc.) or active species (O_3, H_2O_2, etc.) [2]. OH, O, H, N, HO_2, N^+, N_2^+ and O_3 etc. active species with strong reactivity are considered important in removal of acid gases from flue gases, organic compounds removal from water, bacterial decontamination, VOCs decomposition and destruction of other toxic compounds etc. fields [3–12]. Especially, OH radicals play the central role for their strong oxidation in many physicochemical processes [13,14]. In flue gas, NO can be oxidized to NO_2 by O, OH, HO_2 and O_3 and SO_2 can be oxidized to SO_3 by the O atom and the consequent chemical reactions caused by these active species can oxidize those acid gases into H_2SO_4 and HNO_3, and then into aerosol of ammonium sulphate and ammonium nitrate when ammonia is added. Atomic oxygen can react with O_2 to produce ozone. The N atom can convert nitric oxide into molecular nitrogen. Atomic hydrogen plays important roles in chemical vapor depositions of diamond and other functional materials [15,16], plasma etching of thin solid films [17] as well as chemical synthesis of ammonia and other hydrogen-containing compounds [18].

Recently, there have been a number of plasma diagnosis studies regarding the OH, O, H, N, HO_2, N^+, N_2^+ etc. active species [19–30]. Ono and Oda [19–22] had measured the electronic ground state OH radicals generated by a pulsed discharge by laser-induced fluorescence with a tunable KrF excimer laser and discussed the O radical's role to generate OH radicals. Sun et al. [23] did optical studies of radicals (OH, O and H) produced by a pulsed streamer corona discharge in water. The influence of ultraviolet illumination on OH formation in dielectric barrier discharges (DBD) of Ar, O_2 and H_2O mixture was also studied [24]. Su et al. [25] introduced a new method by measuring the amount of CO_2 produced through oxidation of CO by OH radicals for the quantitative measurement of OH. Park et al. [26] investigated additive effect of C_2H_4, H_2O, H_2O_2 on the emission intensity of OH and

[a] e-mail: wangwenc@dlut.edu.cn

$NO/NO_2/NO_x$ reduction and analyzed the related reaction mechanism in corona discharge process using a wire-cylinder plasma reactor. Wang et al. [27] had investigated the emission spectrum of OH, O and H produced in a needle-plate positive pulsed streamer discharge at one atmosphere. Tang et al. [28] present the diagnostic results of N^+ and N_2^+ in high-voltage pulsed corona discharge nitrogen plasma by a molecular beam mass spectrometer. Wang et al. [29,30] also had probed H^-, H_3^-, H^+, H_2^+, H_3^+ etc. ions in dielectric barrier discharge hydrogen plasma by a molecular beam mass spectrometer.

In this article, we present the diagnostic results of OH ($A^2\Sigma \rightarrow X^2\Pi$, 0-0), O ($3p^5P \rightarrow 3s^5S_2^o$), H_α ($3P \rightarrow 2S$) and N ($3p^4P \rightarrow 3s^4S^o$) emission spectra in the high-voltage bi-directional pulsed corona discharge plasma with needle-plate electrode configuration. The bi-directional pulsed corona discharge has a unique advantage over other discharge. Both of positive pulse and negative pulse can produce active species. Horvath and Kiss [31] have pointed out that bi-directional pulsed corona discharge is more efficient than unidirectional pulsed corona discharge in removing NO_x. Especially the removal of contamination in water is more effective [32,33]. The emission spectrum of the $\Delta v = +1$ (1-0, 2-1, 3-2, 4-3) vibration transition band of N_2 ($C^3\Pi_u \rightarrow B^3\Pi_g$) is simulated through gauss distribution. The emission intensity of OH ($A^2\Sigma \rightarrow X^2\Pi$, 0-0) has been evaluated with a satisfactory accuracy. The relative populations of OH ($A^2\Sigma$) radicals and O ($3p^5P$), H_α (3P) and N ($3p^4P$) active atoms have also been obtained by the corresponding emission intensities and Einstein's transition probabilities. The influences of pulse peak voltage, pulse repetition rate and the O_2 flow rate on the relative populations of OH ($A^2\Sigma$) radicals and O ($3p^5P$), H_α (3P) and N ($3p^4P$) active atoms are investigated under severe electromagnetic interference caused by the pulsed discharge. The main involved physicochemical processes have also been discussed.

2 Experimental set-up

The experimental set-up is illustrated schematically in Figure 1a. It is composed of a bi-directional pulsed power supply, a discharge reactor, an optical detection system and a gas-mixing chamber. The bi-directional pulsed power can supply high voltage pulse with a rising time of about 20 ns, a pulse width of about 60 ns, and an adjustable repetition rate in rang of 0–350 Hz. The switch of the bi-directional pulsed power supply is a rotary spark gap and the capacitors used in the pulsed power supply include pulsed capacitor (C_p) and storage capacitor (C). The pulsed capacitor is charged by the storage capacitor and delivers pulse power into the discharge reactor. The schematic diagram of the bi-directional pulse power supply circuit is shown in Figure 1b. The discharge voltage is measured with an oscilloscope (Tektronix TDS3052B) and a 1:1000 high-voltage probe (Tektronix P6015A 1000 × 3.0 pF 100 MΩ). The discharge current is measured with a current probe (Tektronix TCP202). Figure 2a shows the waveform of a bi-directional pulse

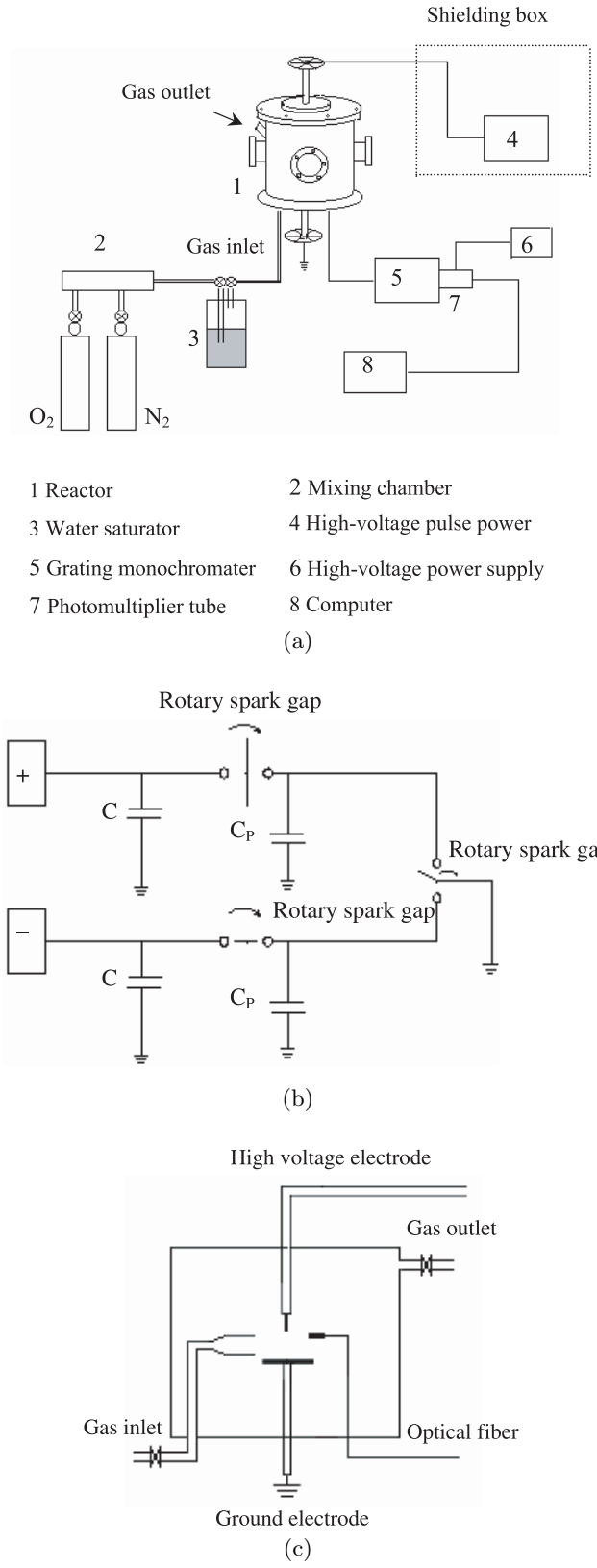

Fig. 1. (a) Schematic of the experimental set-up. (b) The schematic diagram of the bi-directional pulse power supply circuit. The C_P is the pulsed capacitor and the C is the storage capacitor. (c) The detailed drawing of the electrode configuration.

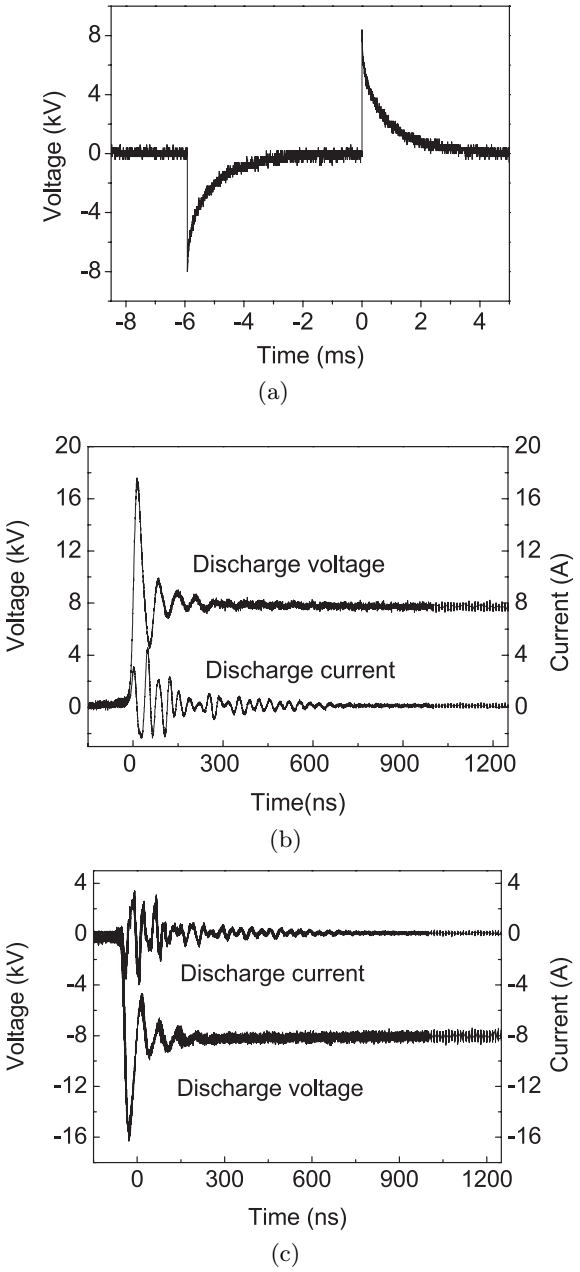

Fig. 2. (a) Typical waveform of the bi-directional pulse discharge voltage in N_2 and water vapor mixture gas. (b) The discharge voltage and discharge current waveforms of the positive pulse of the bi-directional pulse. (c) The discharge voltage and discharge current waveforms of the negative pulse of the bi-directional pulse.

discharge voltage. The waveforms of the positive direction and negative direction of the bi-directional pulse voltage and current are shown in Figures 2b and 2c, respectively. The bi-directional pulsed corona discharge is generated in a stainless-steel reactor so that the environmental conditions could be controlled. The discharge reactor could be evacuated with a rotary pump. The reactor utilizes needle-plate electrode of which can be the 0–30 mm adjustable thickness gas spacing, the needle-plate electrode is placed in the center of the stainless-steel reactor and the discharge plasma is produced in the gas spacing. The positive electrode (needle) is made of tungsten with a diameter of 0.8 mm and the tip of the needle is sharpened and rounded. The cathode is made of a stainless-steel plate with a diameter of 30 mm. A quartz optical fiber head is vertically located 8 mm from the tip of the needle electrode. The gap space between the needle electrode and the plate electrode is fixed at 8 mm. Figure 1c shows the details of the electrode configuration. In order to reduce the interferences of discharge pulses to the detection system and other instruments, the high-voltage pulse power supply is placed in a two-layer shielding box. Both the pulsed power supply and the reactor are connected to the ground separately. The optical emission from the discharge region is collected by a MODEL SP-305 grating monochrometer (grating groove is 1200 lines/mm, glancing wavelength is 350 nm). After the diffraction of the grating, the output spectral light is converted into an electrical signal by a photo multiplication tube (mode R928) and the output of the photo multiplication tube is recorded by a computer. High purity N_2 (99.999%) and high purity O_2 (99.999%) are used as discharge gases under the gas pressure of 1.013×10^5 Pa. The N_2 bubbles the water to control humidity in discharge reactor. The temperature of the water is heated at 100 °C. When the N_2 bubbles through the water and uniformly diffuses into the discharge space, the gas temperature is about 80 °C. The water vapor concentration is about 10% in discharge reactor.

3 Experimental results and discussion

3.1 The measurement of the OH ($A^2\Sigma$) radicals and O ($3p^5P$), H_α (3P) and N ($3p^4P$) active atoms emission spectra

In the non-thermal plasma generated by the bi-directional pulse corona discharge at one atmospheric pressure, electrons with much bigger migration rates can be accelerated by the imposed instantaneous electric field to high kinetic energy. The non-elastic collision of the energetic electrons with H_2O, N_2 and O_2 molecules will induce H_2O, N_2 and O_2 molecules to be dissociated, excited and ionized to produce OH, O, H, N, HO_2, N^+ and O_2^- etc. radicals and active species. Figure 3 shows a typical emission spectrum produced by a bi-directional pulsed corona discharge of N_2 and H_2O mixture at one atmosphere with 31 kV pulse peak voltage and 60 Hz pulse repetition rate. The flow rate of N_2 into the reactor is kept at 200 ml/min. The emission spectrum mainly consists of OH ($A^2\Sigma \rightarrow X^2\Pi$, 0-0), N_2 ($C^3\Pi_u \rightarrow B^3\Pi_g$), O ($3p^5P \rightarrow 3s^5S_2^o$), H_α ($3P \rightarrow 2S$) and N ($3p^4P \rightarrow 3s^4S^o$).

The main physicochemical processes concerning the electrical ground states OH radicals and O, H and N atoms are listed in Table 1.

The main reactions of producing electrical ground states OH radicals and O, H and N atoms in the bi-directional pulse corona discharge N_2 and H_2O plasmas are listed in Table 1. And the excited OH ($A^2\Sigma$) radicals

Table 1. Main physicochemical processes in N_2 and H_2O plasmas.

Reaction process	Reaction rate ($cm^3\ s^{-1}$)[a]	
$e + H_2O \rightarrow e + H + OH$	2.6×10^{-12}	(1)
$e + H_2O \rightarrow H^- + OH$	2.6×10^{-12}	(2)
$e + H_2O \rightarrow 2e + H^+ + OH$	4.4×10^{-16}	(3)
$e + H_2O^+ \rightarrow H + OH$	3.8×10^{-7}	(4)
$O(^1D) + H_2O \rightarrow 2OH$	2.3×10^{-10}	(5)
$N_2\ (A^3\sum_u^+) + H_2O \rightarrow OH+H+N_2$	4.2×10^{-11}	(6)
$e + H_2O \rightarrow 2e + H_2^+ + O$	1.0×10^{-20}	(7)
$e + H_2O^+ \rightarrow H_2 + O$	1.4×10^{-7}	(8)
$e + H_2O^+ \rightarrow 2H + O$	1.73×10^{-7}	(9)
$OH + H \rightarrow H_2 + O$	$1.38 \times 10^{-14}\ T \exp(-3500/T)$	(10)
$e + H_2O \rightarrow 2e + H + OH^+$	2.6×10^{-14}	(11)
$OH + O \rightarrow H + O_2$	3.8×10^{-11}	(12)
$e + N_2 \rightarrow e + 2N$	2.0×10^{-11}	(13)
$e + N_2 \rightarrow 2e + N + N^+$	2.4×10^{-17}	(14)
$e + N^+ \rightarrow N$	3.5×10^{-12}	(15)
$e + N_2^+ \rightarrow 2N$	$2.8 \times 10^{-7}(300/T_e)^{0.5}$	(16)
$N_2 + N_2^+ \rightarrow N^+ + N + N_2$	7.0×10^{-11}	(17)
$N^+ + N_2 \rightarrow N + N_2^+$	$\ll 1.0 \times 10^{-11}$	(18)
$N^+ + O_2 \rightarrow N + O_2^+$	3.0×10^{-10}	(19)
$N_2 + O^+ \rightarrow N + NO^+$	1.2×10^{-12}	(20)
$N_2 + O \rightarrow N + NO$	$1.06 \times 10^{-6} T^{-1} \exp(-38400/T)$	(21)

[a]Rate constants listed here are quoted from reference [34], except for the process (17), (18) which are from reference [28]. The rate constants refer to the mean electronic energy kT_e of 3.3 eV for electron-involved interactions or T_{ion} ($\approx T_{neutr}$) of 300 K for neutral-ion reactions, except for process (10), (16) and (21), where T represents the gas temperature involved in the expression.

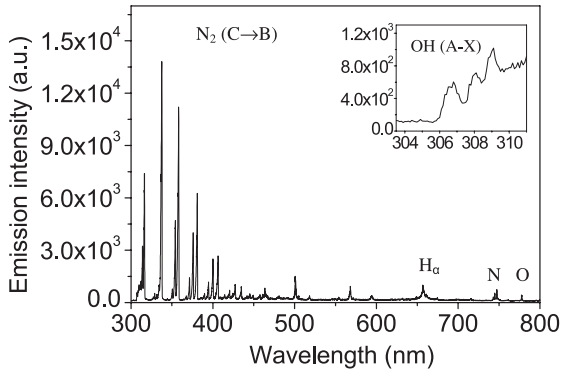

Fig. 3. Typical emission spectra of OH ($A^2\Sigma \rightarrow X^2\Pi$ 0-0), N_2 ($C^3\Pi_u \rightarrow B^3\Pi_g$), O ($3p^5P \rightarrow 3s^5S_2^o$), H_α (3P → 2S) and N ($3p^4P \rightarrow 3s^4S^o$) generated by a bi-directional pulsed corona discharge in N_2 and H_2O mixture at 31 kV pulse peak voltage and 60 Hz pulse repetition rate.

and O ($3p^5P$), H_α (3P) and N ($3p^4P$) active atoms are also mainly produced by the reactions in Table 1. The probability of the interactions of electrons and electrical ground states radicals is very little for the small concentrations of the ground states radicals and the interactions can be neglected.

Therefore, at the present experimental conditions, OH ($A^2\Sigma$) radicals are mainly produced in reactions (1) and (2) by the electron-molecule interactions of electrons and H_2O and the reactions (3–6) can be neglected for the small concentrations of H_2O^+, O (^1D) and $N_2(A^2\Sigma_u^+)$ and little reaction rates.

The reactions (7–10) can produce O ($3p^5P$) atoms, nevertheless the reactions of (8–10) are unlikely dominant for the production of O ($3p^5P$) atoms due to the small concentrations of H_2O^+, OH and H. Therefore, O ($3p^5P$) atoms are predominantly formed in reaction (7) by the electron-molecule interaction of electrons and H_2O.

Similarly, the reactions (4), (6), (9), (11) and (12) are unlikely dominant for the production of H_α (3P) atoms due to the small concentration of H_2O^+, $N_2(A^2\Sigma_u^+)$, OH and O as well as small rate constant in reactions, thus, the electron-molecule interaction (1) of electron and H_2O is likely the most important.

N ($3p^4P$) atoms can be formed in reactions (13–21). While the reactions (14–21) are unlikely dominant in N_2 and H_2O plasmas due to the small concentration of N_2^+, N^+, O, O^+ and O_2 as well as small rate constant in reactions. The electron-molecule interaction (13) of electron and N_2 is the predominant process to produce N ($3p^4P$) atoms.

3.2 The relative vibrational populations and the vibrational temperature of N_2 (C, v′)

Figure 4 is a part of Figure 3. From Figure 4 we can see that the emission spectrum of OH ($A^2\Sigma \rightarrow X^2\Pi$, 0-0) is seriously interfered by the emission spectrum of

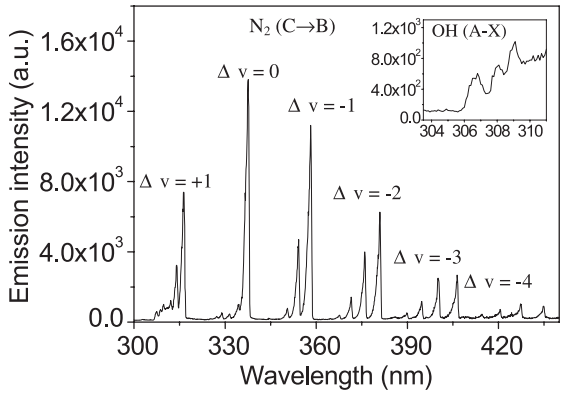

Fig. 4. Typical emission spectra of OH ($A^2\Sigma \rightarrow X^2\Pi$ 0-0) and N_2 ($C^3\Pi_u \rightarrow B^3\Pi_g$) generated by a bi-directional pulsed corona discharge in N_2 and H_2O mixture at 31 kV pulse peak voltage and 60 Hz pulse repetition rate.

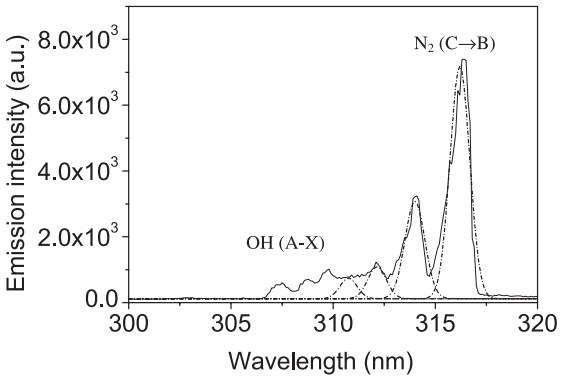

Fig. 5. The emission intensity of OH ($A^2\Sigma \rightarrow X^2\Pi$ 0-0) obtained through the simulation of the emission spectrum of the $\Delta v = +1$ vibration transition band of N_2 ($C^3\Pi_u \rightarrow B^3\Pi_g$) by the Gauss form and the relative populations of N_2 (C, v').

the $\Delta v = +1$ vibration transition band of N_2 ($C^3\Pi_u \rightarrow B^3\Pi_g$). Therefore, it is necessary to subtract the emission intensity of the $\Delta v = +1$ vibration transition band of N_2 ($C^3\Pi_u \rightarrow B^3\Pi_g$) from the overlapping spectra to get the emission intensity of OH ($A^2\Sigma \rightarrow X^2\Pi$, 0-0). The relative vibrational populations of N_2 (C, v') can be determined though the equation (22):

$$S_{v'v''} \propto N_{v'}(FC)_{v'v''}R_e^2(r_{v'v''})\nu_{v'v''}^3 \qquad (22)$$

where $S_{v'v''}$ is the integral emission intensity, $N_{v'}$ is the population of the electronic excitation state vibrational energy level $v', (FC)_{v'v''}$ is the corresponding Frank-Condon factor (quoted from Ref. [35]), $R_e(r_{v'v''})$ is electronic transition moment and $R_e(r_{v'v''})$ is nearly constant, $\nu_{v'v''}$ is the corresponding transition frequency. By calculating the integral emission intensity $S_{v'v''}$ of the $\Delta v = -3$ and the $\Delta v = -4$ vibration transition bands of N_2 ($C^3\Pi_u \rightarrow B^3\Pi_g$), the relative vibrational populations of N_2 (C, v') in present experimental condition can be determined N_0:N_1:N_2:N_3:N_4 = 1.00:0.384:0.116:0.044:0.019 by equation (22). And then the vibrational temperature of N_2 (C) can be determined by the following equation:

$$N_1/N_0 = e^{-\Delta E/kT_v} \qquad (23)$$

where N_1 and N_0 are the relative vibrational populations of the 1 and 0 vibrational states, respectively. ΔE is the energy difference between the 1 and 0 vibrational states and k is the Boltzman's constant. T_v stands for the vibrational temperature. Therefore, the vibrational temperature between the 1 and 0 vibrational states can be determined, and the vibrational temperatures between the 2 and 1, 3 and 2, 4 and 3 vibrational states also can be determined with the same method. At present experimental conditions, the mean vibrational temperature of N_2(C) is 2790 K.

The emission intensity of the $\Delta v = +1$ (1-0, 2-1, 3-2, 4-3) vibration transition band of N_2 ($C^3\Pi_u \rightarrow B^3\Pi_g$) can be determined by equation (22) with the relative vibrational populations of N_2 (C, v'), Frank-Condon factor and the spectrum response of photomultiplier tube. Since the experimental pressure is at one atmosphere, gas molecule collision frequency is about 10^{10} times per second by gas dynamics. The radiation lifetime of the N_2 (C) state is about 40 ns [35], therefore the N_2 (C) molecule collides with other gas molecules about 400 times before radiative emission. The rotational equilibrium is reached in each vibrational state of the N_2 (C) state, and then the vibrational distribution can be described by the same expression. Due to the difficulty of determining the exact emission spectrum line shape function, a Gaussian form was used for the deconvolution of the overlapping emission spectrum (Fig. 5). The emission spectrum of the $\Delta v = +1$ (1-0, 2-1, 3-2, 4-3) vibration transition band of N_2 ($C^3\Pi_u \rightarrow B^3\Pi_g$) can be deduced quite accurately from the simulation process. And then the emission intensity of OH ($A^2\Sigma \rightarrow X^2\Pi$, 0-0) can be evaluated with a satisfactory accuracy by subtracting the emission intensity of the $\Delta v = +1$ vibration transition band of N_2 ($C^3\Pi_u \rightarrow B^3\Pi_g$) from the overlapping spectra.

The relation between the emission intensity S and the excited state relative population is given as follows

$$S = NAh\nu \qquad (24)$$

where A is the Einstein's transition probability, h is the Planck constant, ν is the transition frequency. Therefore, the relative population of OH ($A^2\Sigma$) can be determined by equation (24) with the emission intensity of OH ($A^2\Sigma \rightarrow X^2\Pi$, 0-0) and the corresponding Einstein's transition probabilities (A(OH) = 0.0145×10^8 s^{-1}, A(O) = 1×10^8 s^{-1}, A(H) = 0.225×10^8 s^{-1}, A(N) = 0.193×10^8 s^{-1}).

3.3 The effects of pulse peak voltage on the relative populations of OH ($A^2\Sigma$) radicals and O ($3p^5P$), H_α (3P) and N ($3p^4P$) active atoms

The effects of pulse peak voltage on the relative populations of OH ($A^2\Sigma$) radicals and O ($3p^5$P), H_α (3P) and N ($3p^4$P) active atoms are shown in Figure 6. The pulse repetition rate is 60 Hz and is kept constant during the

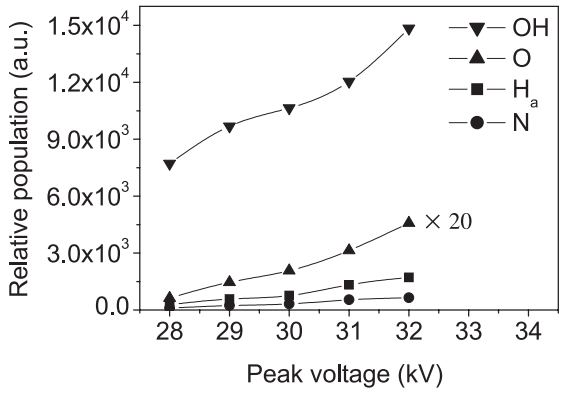

Fig. 6. The relative populations of OH ($A^2\Sigma$) radicals and O ($3p^5$P), H_α (3P) and N ($3p^4$P) active atoms as a function of pulse peak voltage at 60 Hz pulse repetition rate and one atmosphere.

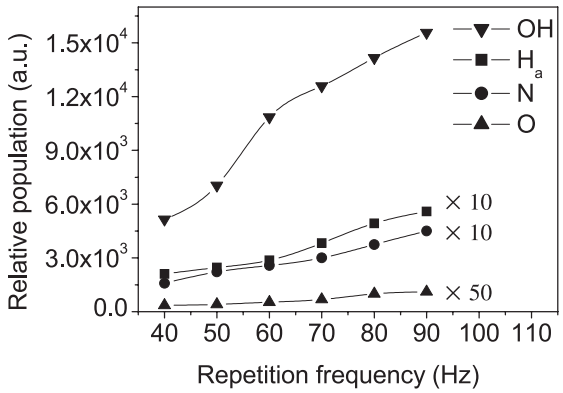

Fig. 7. The relative populations of OH ($A^2\Sigma$) radicals and O ($3p^5$P), H_α (3P) and N ($3p^4$P) active atoms as a function of pulse repetition rate at 30 kV pulse peak voltage and one atmosphere.

measurements. The flow rate of N_2 into the reactor is kept at 200 ml/min. Figure 6 clearly shows that the relative populations of OH ($A^2\Sigma$) radicals and O ($3p^5$P), H_α (3P) and N ($3p^4$P) active atoms increase with increasing pulse peak voltage.

The OH ($A^2\Sigma$) radicals and O ($3p^5$P), H_α (3P) and N ($3p^4$P) active atoms are mainly produced by the electron-molecule interactions (1), (2), (7) and (13). The increasing of pulse peak voltage can induce the increasing of the high-energy electron density and the electron mean energy and more OH ($A^2\Sigma$) radicals and O ($3p^5$P), H_α (3P) and N ($3p^4$P) active atoms can be produced by the electron-molecule interactions (1), (2), (7) and (13). Therefore, the populations of OH ($A^2\Sigma$) radicals and O ($3p^5$P), H_α (3P) and N ($3p^4$P) atoms increase with the increasing of pulse peak voltage.

3.4 The effects of pulse repetition rate on the relative populations of OH ($A^2\Sigma$) radicals and O ($3p^5$P), H_α (3P) and N ($3p^4$P) active atoms

The effects of pulse repetition rate on the relative populations of OH ($A^2\Sigma$) radicals and O ($3p^5$P), H_α (3P) and N ($3p^4$P) active atoms are shown in Figure 7. The pulse peak voltage is 30 kV and is kept constant during the measurements. The flow rate of N_2 into the reactor is kept at 200 ml/min. From Figure 7, we can see that the relative populations of those excited states radicals increase with increasing pulse repetition rate. Since the peak voltage is not changed, per unit pulse discharge creates nearly the same number of radicals and active atoms. Thus the relative populations of OH ($A^2\Sigma$) radicals and O ($3p^5$P), H_α (3P) and N ($3p^4$P) atoms increase with the increasing of pulse repetition rate.

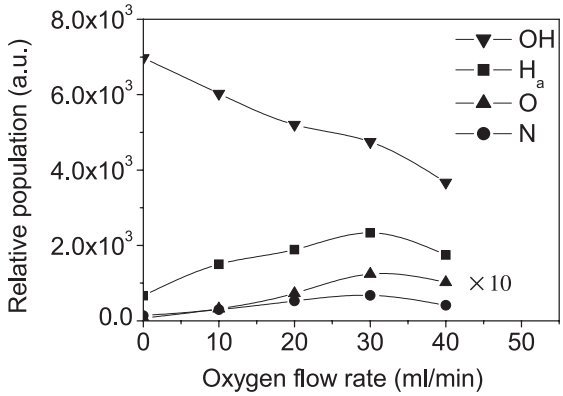

Fig. 8. The relative populations of OH ($A^2\Sigma$) radicals and O ($3p^5$P), H_α (3P) and N ($3p^4$P) active atoms as a function of O_2 flow rate at 29 kV pulse peak voltage and 70 Hz pulse repetition rate.

3.5 The effects of O_2 addition on the relative populations of OH ($A^2\Sigma$) radicals and O ($3p^5$P), H_α (3P) and N ($3p^4$P) active atoms

In order to investigate the effects of oxygen on the relative populations of OH ($A^2\Sigma$) radicals and O ($3p^5$P), H_α (3P) and N ($3p^4$P) active atoms, oxygen is added into the N_2 and H_2O mixture in the bi-directional pulsed corona discharge. When oxygen is added, the added O_2 capture a lot of free electrons and form O_2^- ions and the humidity enhances the attachment of electrons to O_2, thus the added O_2 decrease greatly the density of free electrons and the electron mean energy [36–38]

$$e + O_2 \rightarrow O_2^- \tag{25}$$

$$e + O_2 + M \rightarrow O_2^- + M \tag{26}$$

where M may be N_2, O_2, and H_2O molecule.

Figure 8 clearly shows that the relative populations of OH ($A^2\Sigma$) radicals and O ($3p^5$P), H_α (3P) and N ($3p^4$P) active atoms varies as a function of O_2 flow rate at 4 different oxygen flow rates of 10, 20, 30 and 40 ml/min at

29 kV pulse peak voltage and 70 Hz pulse repetition rate. The flow rate of N_2 into the reactor is kept at 200 ml/min. From Figure 8, we can see that the relative population of OH ($A^2\Sigma$) decreases with the flow rate of oxygen. The relative populations of O ($3p^5P$), H_α (3P) and N ($3p^4P$) active atoms increase with the flow rate of oxygen at first (from 0 to 30 ml/min) and exhibit a maximum value at about 30 ml/min. When the flow rate of oxygen is increased further, the relative populations of those active atoms decrease correspondingly.

In order to explain the observed experimental phenomena, we will further discuss the physicochemical processes of interaction when oxygen is added. Firstly the added O_2 can be dissociation in the reactions (27–29) by the electron-molecule interactions of electrons and O_2:

$$e + O_2 \rightarrow O^- + O \tag{27}$$

$$e + O_2 \rightarrow e + O + O\left(^1D\right) \tag{28}$$

$$e + O_2 \rightarrow O^+ + O + 2e. \tag{29}$$

A lot of excited state O ($3p^5P$) atoms and O (^1D) can be produced. Ono and Oda [21] have pointed out that in a humid air, most of the OH would be produced by interaction of O (^1D) and H_2O in reaction (5). And Penetrante [38] also points out that when O_2 exists and forms water cluster ions ($O_2^+(H_2O)$ and $H_3O^+(H_2O)$) it is an important approach to form OH radicals through the dissociative reactions of water cluster ions

$$O_2^+(H_2O) + H_2O \rightarrow H_3O^+ + OH + O_2 \tag{30}$$

$$H_3O^+(OH) + H_2O \rightarrow H_3O^+ + OH + H_2O. \tag{31}$$

Thus, a lot of OH radicals can be produced. However, at the same time, a lot of O atoms and O_3 molecules produced by the added O_2 can react with OH radicals

$$OH + O \rightarrow H + O_2 \tag{12}$$

$$OH + O_3 \rightarrow HO_2 + O_2. \tag{32}$$

Because of the depletion of OH radicals and free electrons, the relative population of excited state OH ($A^2\Sigma$) radicals decrease with increasing the added O_2 flow rate.

At the same time, a lot of excited state H_α (3P) atoms can be produced by interaction of OH and O by reaction (12). Owing to the concentrations of O_2, O and O^+ rising obviously when oxygen flow is added into a N_2 and H_2O mixture, more excited state N ($3p^4P$) atoms also can be produced by the reactions (19), (20) and (21).

Thus it can be seen, when the oxygen flow is added into N_2 and H_2O mixture, the relative populations of O ($3p^5P$), H_α (3P) and N ($3p^4P$) active atoms enhance at the beginning. When the flow rate of oxygen is increased further, the added O_2 capture lots of electrons and form O_2^- ions by the processes (25) and (26) and the density of free electrons and the electron mean energy are decreased greatly. When oxygen depletes too many free electrons in the discharge, the discharge channels are seriously destroyed and the relative populations of O ($3p^5P$), H_α (3P) and N ($3p^4P$) active atoms decrease.

For further understanding of the observed phenomena and the mechanism involved, a relatively detailed dynamics simulation is underway and will be reported later.

4 Conclusions

In this study, we have successfully recorded the emission spectra of OH ($A^2\Sigma \rightarrow X^2\Pi$, 0-0), O ($3p^5P \rightarrow 3s^5S_2^o$), H_α ($3P \rightarrow 2S$) and N ($3p^4P \rightarrow 3s^4S^o$) in the bi-directional pulse corona discharge with a needle-plate electrode at one atmosphere. The severe electromagnetic interference caused by the bi-directional pulse corona discharge itself has been overcome by double shielding and specially designed multiple grounding of the discharge source and the reactor. The relative vibrational populations and the vibrational temperature of N_2 (C, v') have been determined. The emission spectrum of the $\Delta v = +1$ (1-0, 2-1, 3-2, 4-3) vibration transition band of N_2 ($C^3\Pi_u \rightarrow B^3\Pi_g$) is simulated through gauss distribution. The emission intensity of OH ($A^2\Sigma \rightarrow X^2\Pi$, 0-0) has been evaluated with a satisfactory accuracy by subtracting the emission intensity of the $\Delta v = +1$ vibration transition band of N_2 ($C^3\Pi_u \rightarrow B^3\Pi_g$) from the overlapping spectra. The relative populations of OH ($A^2\Sigma$) radicals and O ($3p^5P$), H_α (3P) and N ($3p^4P$) active atoms have been obtained by the corresponding emission intensity and Einstein's transition probabilities. It is found that the relative populations of OH ($A^2\Sigma$) radicals and O ($3p^5P$), H_α (3P) and N ($3p^4P$) active atoms increase with increasing the pulse peak voltage and the pulse repetition rate. When the different oxygen flows are added in N_2 and H_2O mixture gas, the relative population of OH ($A^2\Sigma$) radicals decreases with increasing the flow rate of oxygen. The relative populations of O ($3p^5P$), H_α (3P) and N ($3p^4P$) active atoms increase with the flow rate of oxygen at first and exhibit a maximum value at about 30 ml/min. When the flow rate of oxygen is increased further, the relative populations of those excited states active atoms decrease correspondingly.

The author would like to thank professor Xuechu Li for friendly discussion and suggestion. This work is supported by the united fund of the National Natural Science Foundation Committee of China and Engineering Physical Institute of China granted under No. 10276008 and the fund of Liaoning Province Natural Science Foundation Committee granted under No. 20022138.

References

1. A. Mizuno, J.S. Clements, R.H. Davis, IEEE Trans. Ind. Appl. **22**, 516 (1986)
2. R.P. Dahiya, S.K. Mishra, A. Veefkind, IEEE Trans. Plasma Sci. **21**, 346 (1993)
3. A.T. Sugiarto, S. Ito, T. Ohshima, M. Sato, J.D. Skalny, J. Electrostat. **58**, 135 (2003)
4. J.J. Lowke, R. Morrow, IEEE Trans. Plasma Sci. **23**, 661 (1995)

5. A. Abou-Ghazala, S. Katsuki, K.H. Schoenbach, F.C. Dobbs, K.R. Moreira, IEEE Trans. Plasma Sci. **30**, 1449 (2002)
6. M. Yamamoto, M. Nishioka, M. Sadakata, J. Electrostat. **56**, 173 (2002)
7. T. Oda, J. Electrostat. **57**, 293 (2003)
8. U. Roland, F. Holzer, F.D. Kopinke, Catal. Today **73**, 315 (2002)
9. N.M. Šišović, G.Lj. Majstorović, N. Konjević, Eur. Phys. J. D **32**, 347 (2005)
10. W. Ebeling, H. Hache, M. Spahn, Eur. Phys. J. D **23**, 265 (2003)
11. K.P. Yan, E.J.M. van Heesch, A.J.M. Pemen, P.A.H.J. Huijbrechts J. Electrostat. **51-52**, 218 (2001)
12. F. Liu, W.C. Wang, S. Wang, C.S. Ren, Y.N. Wang, Plasma Sci. Technol. **7**, 2851 (2005)
13. V.A. Lozovsky, I. Derzy, S. Cheskis, Chem. Phys. Lett. **284**, 407 (1998)
14. A.A. Joshi, B.R. Locke, P. Arce, W.C. Finney, J. Hazard. Mater. **41**, 3 (1995)
15. S.S. Lee et al., Science **263**, 1596 (1994)
16. A. Gijcquel et al., Cur. Appl. Phys. **1**, 479 (2001)
17. H. Umemoto et al., J. Non-Cryst. Sol. **299-302**, 9 (2002)
18. H. Kiyooka, O. Matsumoto, Plasma Chem. Plasma Proc. **16**, 547 (1996)
19. R. Ono, T. Oda, IEEE Trans. Ind. Appl. **37**, 709 (2001)
20. R. Ono, T. Oda, IEEE Trans. Ind. Appl. **36**, 82 (2000)
21. R. Ono, T. Oda, in *Proceedings of Thirty-Fourth IAS Annual Meeting, Industry Applications Conference, Conference Record of the 1999 IEEE.* **3** (1999), p. 1461
22. R. Ono, T. Oda, J. Phy. D: Appl. Phys. **35**, 2133 (2002)
23. B. Sun, M. Sato, A. Harano, J.S. Clements, J. Electrostat. **43**, 115 (1998)
24. Z. Falkenstein, J. Appl. Phys. **81**, 7158 (1997)
25. Z. Su, H.H. Kim, M. Tsutsui, K. Takashima, A. Mizuno, in *Proceedings of Thirty-Fourth IAS Annual Meeting, Industry Applications Conference, Conference Record of the 1999 IEEE.* **3** (1999), p. 1473
26. C.W. Park, J.W. Hahn, D.N. Shin, in *Proceedings of the Pacific Rim Conference on Lasers and Electro-Optics. CLEO/Pacific Rim '1999.* **2** (1999), p. 356
27. W.C. Wang, F. Liu, J.L. Zhang, C.S. Ren, Spectrosc. Spect. Anal. **24**, 1288 (2004) (in Chinese)
28. S.K. Tang et al., J. Vac. Sci. Technol. A **18**, 2213 (2000)
29. W.C. Wang et al., Chem. Phys. Lett. **377**, 512 (2003)
30. W.C. Wang et al., J. Phys. D: Appl. Phys. **37**, 1185 (2004)
31. M. Horvath, E. Kiss, J. Electrostat. **63**, 993 (2005)
32. R.B. Zhang, Y. Wu, C.Y. Jin, J. Li, J. Dal. Univ. Technol. **43**, 719 (2003)
33. R.B. Zhang, Y. Wu, C.Y. Jin, J. Li, J. Zhongyuan Inst. Technol. **14**, 36 (2003)
34. O. Eichwald et al., J. Appl. Phys. **82**, 4781 (1997)
35. S.N. Suchard, *Spectroscopic Data: Vol. 1, Homonuclear Diatomic Molecules Part B* (The Aerospace Corporation Los Angeles, California, 1975)
36. W.C. Wang, F. Liu, J.L. Zhang, Y.N. Wang, Spectrochimica Acta A **59**, 3267 (2003)
37. W.C. Wang, J.L. Zhang, F. Liu, Y. Liu, Y.N. Wang, Vacuum **74**, 333 (2004)
38. B.M. Penetrante, J.N. Bardsley, M.C. Hsiao, Jpn J. Appl. Phys. **36**, 5007 (1997)